PERFORMANCE ANALYSIS OF ORGANIC RANKINE CYCLES USING HFC- AND HC-BASED ZEOTROPIC MIXTURES UNDER DIFFERENT HEAT SOURCE TEMPERATURES

Jui-Ching Hsieh[1]*, Chung-Cheng Yeh[2], Hsuah-Cheng Liu[3], Wen-Chieh Wu[4], Wei-Hung Shih[5]

[1]Department of Mechanical Engineering, National Chin-Yi University of Technology, Taichung, Taiwan
jchsieh@ncut.edu.tw
[2] Department of Mechanical Engineering, National Chin-Yi University of Technology, Taichung, Taiwan
rnes20420@gmail.com
[3] Metal Industries Research & Development Centre, Kaohsiung, Taiwan
hcliu98@mail.mirdc.org.tw
[4] Metal Industries Research & Development Centre, Kaohsiung, Taiwan
wcwu@mail.mirdc.org.tw
[5] Metal Industries Research & Development Centre, Kaohsiung, Taiwan
weihung.shih@mail.mirdc.org.tw

ABSTRACT

Owing to growing industrialization, the energy consumption has increased considerably over the past few decades, which has led as acid rain, ozone layer depletion, and global warming. Most industries exhaust a lot of low-grade heat to environment. ORC (organic Rankine cycle) is one of effective methods for conversion of low-grade heat into electricity. Conversion efficiency of ORC is significantly affected by the temperature difference between heating and cooling source, and working fluids. Actually, working fluids cause great damage on the environment, especially for high global warming potential (GWP). Hydro-fluorocarbon (HFC) refrigerants with high GWP are widely used as working fluids in ORC owing to their excellent thermodynamic properties. By contrast, hydro-carbon (HC) refrigerants have low GWP and high flammability, and they're suitable in high and medium temperature of the heat source. To achieve high conversion efficiency of system and low GWP of working fluids, HFCs, HCs and HFO could be mixed to use as working fluid in ORC. The purpose of the present study was to develop a thermodynamic analysis model by using MATLAB and investigate feasibility of HFC/HC and HFC/HFO mixtures instead of HFC/HFC at heat source temperature 100 ℃ − 210 ℃. The results indicate optimal mole fractions corresponding to the maximal thermal efficiency and specific power were not and notably affected by $T_{h,in}$, respectively. Furthermore, the thermal efficiency and specific power were slightly decreased and substantially increased with an increase $T_{h,in}$. Finally, the R600a/R134a and R600a/R290 at optimal mole fraction can operate with a low GWP and a relatively high specific power comparing to the mixtures.

1. INTRODUCTION

Due to the development of industrialization, the environment pollution has become a severe challenge to the world. The organic Rankine cycle (ORC) is one of the effective technologies, which used to convert low-medium grade heat energy into power (Wei, 2007), (Desai and Bandyopadhyay, 2009). However, ORC performance is notably affected by evaporating and condensing temperature, and working fluid. Selection of working fluid was carried out to investigate effect of evaporation parameters on ORC performance (Papadopoulos, 2010). Wang *et al*. (2009) investigated that the cycle has the highest exergy efficiency by using R236EA as working fluid. In addition, Gao *et al*. (2016) showed that the considered working fluids have a critical temperature about 40-65℃ lower than the inlet temperature of flue gas in supercritical ORC system. For subcritical ORC system, the working fluids with low evaporation latent heat and high liquid specific heat can generate higher net power output. Tchanche *et al*. (2009) demonstrate that R134a, R152a, R600, R600a are the most suitable

fluids for small scale solar applications. However, R152a, R600, R600a are limited because of the flammability. To improve the ORC efficiency, some studies have focused on using zeotropic mixture as working fluid at various temperatures. Heberle *et al*. (2012) used isobutene/isopentane and R227ea/R245fa to carry out the detailed simulation and analysis at the heat source temperature of 120℃. They pointed out that the system efficiency could reach 4.3%~15% for the zeotropic mixtures compared with pure refrigerant. Borsukiewicz-Gozdur and Nowak (2007) found that the power output of the ORC using propane/ethane was higher than that of the pure propane. Wang and Zhao (2009) investigated three mass fractions of R245fa/R152a at fixed evaporation and condensation temperature. The results showed that the volume flow rate of R245fa/R152a at the inlet of the expander was lower with respect to pure R245fa to reduce the turbine dimensions and costs. Sadeghi *et al*. (2016) indicated that using zeotropic mixtures as working fluid can instead the pure fluid such as R245fa in ORC, PTORC(parallel two-stage evaporator organic Rankine cycle), STORC(series two-stage evaporator organic Rankine cycle). Wang *et al*. (2016) selected R601a/R600a as working fluid, the results showed that the maximum net power appear at 0.6/0.4(mass fraction) at the heat source temperature of 115°C, besides, The net power output of R601a/R600a (0.6/0.4) is higher than that of R601a by 25%. Dong *et al*. (2018) discussed the effects of heat source temperature and mixture mass fraction on the net power output, heat exchanger size, and cost-effective performance by using pure fluid and zeotropic mixtures, include R245fa, R245ca, R123, R365mfc and R113, the results showed that zeotropic ORC is capable of producing more net power than pure ORC, particularly for heat source with larger temperature difference.

Although hydrofluorocarbons refrigerants, namely R245 and R134a, are popular and widely used as working fluid in ORC system, they have high GWP. Hydrocarbon refrigerants (R290 and R600a), which with low GWP and higher flammability, are environmentally friendly, non-toxic and non-ozone-depleting. The present work aimed to investigate the performance of HFC/HC and HFC/HFO with low greenhouse effect to explore feasibility of they instead of HFC/HFC. Therefore, in the present study, a thermodynamic model of ORC was built and the mole fraction of the mixtures were optimized to obtain maximum thermal efficiency and specific power at various heat source temperatures.

2. Thermodynamic method

The ORC system applies the same principle as the traditional Rankine cycle which used water as working fluid. The present ORC model was simulated for typical geothermal heat sources in Taiwan. In the present study, R290, R134a and R1234yf with low GWP were mixed with R245fa and R600a with high GWP, respectively. In addition, the thermodynamic properties of the working fluids referred from database Lemmon *et al*. (2010) are listed in Table 1.

Table 1 Physical and environmental data of working fluids

Substance	Physical data				Environmental data		Fluid type
	Molecular weight (g/mol)	T_{cri} (℃)	T_b (℃)	P_{cri} (MPa)	ODP	GWP (100yr)	
R245fa	134.05	154.01	15.14	3.65	0	1003	Dry
R1234yf	114.04	94.7	-29.45	3.38	0	4	Dry
R134a	102.03	101.1	-26.07	4.06	0	1430	Wet
R290	44.10	96.69	-42	4.25	0	3	Wet
R600a	58.12	134.7	-11.74	3.64	0	~20	Isentropic

2.1 System description

As shown in Fig. 1, a typical ORC consists of a feeding pump, an evaporator, an expander, and a condenser. The cycle can be divided into four processes. First of all, the working fluid leaves the condenser and is pressurized by pump as a sub-cooled liquid (process 1-2). Second, the working fluid flows into the evaporator to be heated by external heat sources (process 2-5), such as solar heat, waste heat or geothermal energy. Third, the high-pressure vapor flows into the expander to generate electricity (process 5-6). Finally, the low-pressure vapor exits the expander into condenser, thereafter, the vapor is condensed by cooling source (process 6-1).

2.2 Design conditions

The temperature-specific entropy (T-s) diagram and system design conditions are shown in Fig. 2 and Table 2, respectively. The inlet temperature of the heat source was ranged from 100 ℃ to 210 ℃ and the inlet temperature of cooling source was 32 ℃. The mass flow rate for the heat source was set at 1 kg/s. Furthermore, the isentropic efficiencies for the pump and expander, and the motor and generator were assumed at 65% and 80%, and 90% and 90 %, respectively.

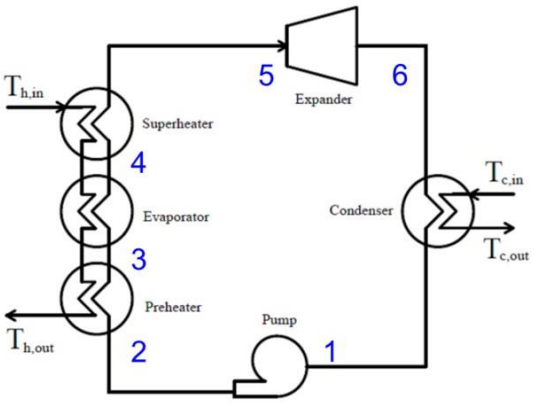

Fig. 1 Configuration and processes of ORC system

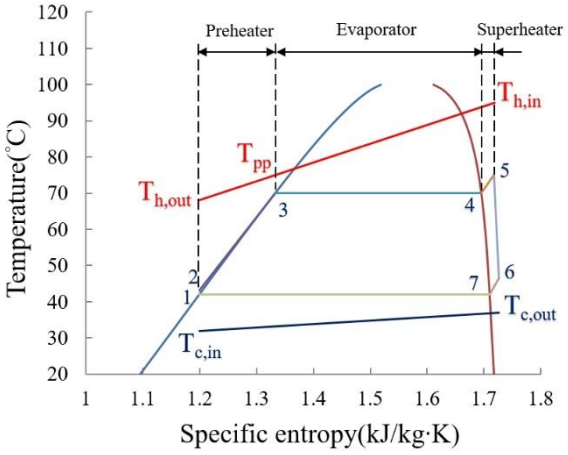

Fig. 2 Schematic T-s diagram of the system

Table 2 Given parameters of the ORC system

Items	Parameters	Assumption
Heat source temperature	$T_{h,in}$	100 ~ 210 ℃
Cooling source temperature	$T_{c,in}$	32 ℃
Temperature of evaporation	T_{evap}	70 ℃
Temperature difference of pinch point in the evaporator	$\Delta T_{pp,evap}$	5 K
Temperature difference of pinch point in the condenser	$\Delta T_{pp,cond}$	5 K
Mass flow rate of heat source	$\dot{m}_h$	1 kg/s
Pump isentropic efficiency	η_p	65 %
Expander isentropic efficiency	η_{exp}	80 %
Motor/generator efficiency	η_m, η_{gen}	90 %

2.3 Energy analysis

Energy analysis model is based on the thermal efficiency of thermodynamics which is used to describe a statement of the conservation of energy. The energy analysis of each process can be expressed as following:

- Pumping process
  - Pump isentropic efficiency

$$\eta_s^p = \frac{h_{2s}-h_1}{h_2-h_1} \quad (1)$$

  - Pumping power consumption

$$\dot{W}_p = \dot{m}_{wf}(h_2 - h_1) \quad (2)$$

  - Pumping electrical consumption

$$\dot{W}_p^{elec} = \dot{W}_p/\eta_m \quad (3)$$

- High-temperature heat transfer process

$$\dot{Q}_h = \dot{m}_h\left(h_{h,in} - h_{h,out}\right) = \dot{m}_{wf}(h_5 - h_2) \quad (4)$$

- Expansion process

- Expander isentropic efficiency

$$\eta_s^{exp} = \frac{h_5 - h_6}{h_5 - h_{6s}} \quad (5)$$

- Expander shaft power output

$$\dot{W}_{exp} = \dot{m}_{wf}(h_5 - h_6) \quad (6)$$

- Expander electrical power output

$$\dot{W}_{exp}^{elec} = \dot{W}_{exp}\eta_{gen} \quad (7)$$

■ Condensation process

$$\dot{Q}_c = \dot{m}_c\left(h_{c,out} - h_{c,in}\right) = \dot{m}_{wf}(h_6 - h_1) \quad (8)$$

■ System efficiency

- Net mechanical power output

$$\dot{W}_{net} = \dot{W}_{exp} - \dot{W}_p \quad (9)$$

- Net electrical power output

$$\dot{W}_{net}^{elec} = \dot{W}_{exp}^{elec} - \dot{W}_p^{elec} \quad (10)$$

- Thermal efficiency of thermodynamics

$$\eta_I = \frac{\dot{W}_{net}}{\dot{Q}_h} \quad (11)$$

- Specific power

$$\xi = \frac{\dot{W}_{net}^{elec}}{\dot{m}_h} \quad (12)$$

2.4 Verification of analysis model

To validate the thermodynamic analysis model developed in the present study, the model was solved with the same operating conditions and working fluid as those in Le *et al.* (2014). According to the validation results, the relative deviations in the first and second law efficiencies are within 2 %, as listed in Table 3.

Table 3 Verification of the ORC model.

Substance	η_I (%)			η_{II} (%)		
	Ref. Le *et al.* (2014)	Present study	Deviation (%)	Ref. Le *et al.* (2014)	Present study	Deviation (%)
R245fa/Pentane(0/1)	14.6	14.56	0.27	53.2	52.81	0.73
R245fa/Pentane(0.3/0.7)	12.6	12.40	1.59	46.4	45.79	1.31
R245fa/Pentane(0.4/0.6)	12.6	12.43	1.35	47.2	46.46	1.57
R245fa/Pentane(0.5/0.5)	12.8	12.68	0.94	48.5	48.03	0.97
R245fa/Pentane(0.6/0.4)	13.0	13.02	0.15	50.2	50.12	0.16
R245fa/Pentane(0.7/0.3)	13.2	13.20	0	51.8	51.69	0.21
R245fa/Pentane(1/0)	13.7	13.66	0.29	53.0	52.97	0.06

3. Results and discussions

The thermodynamic model of ORC has been developed by using MATLAB software to evaluate performance of HFC/HC, HFC/HFO and HFC/HFC at various heat source temperatures. To this purpose, the analysis has been carried out adopting R245fa/R290, R245fa/R134a, R245fa/R1234yf, R600a/R290, R600a/R134a and R600a/R1234yf as working fluid and the evaporating temperature is 70 °C. Additionally, the thermal efficiency and specific power of pure fluids are shown in Table 4.

3.1 Optimal mole fraction

In the present study, the six zeotropic mixtures, namely R245fa/R290, R245fa/R134a, R245fa/R1234yf, R600a/R290, R600a/R134a and R600a/R1234yf, were used as working fluids to

investigate optimal mole fraction at various $T_{h,in}$. The optimal mole fractions of the mixtures corresponding to the maximal thermal efficiency and the specific power at various $T_{h,in}$ are shown in Table 5. As shown in Table 5, the thermal efficiency and specific power lower than zeotropic mixtures by using pure fluid as working fluid. Therefore, zeotropic mixtures may consider to be the working fluid in present study. The optimal mole fraction corresponding to maximal thermal efficiency was not substantially affected by $T_{h,in}$. However, the optimal mole fraction corresponding to the maximal specific power was notably changed as $T_{h,in}$ higher than 180 ℃, except R245fa/R290 and R600a/R290. There were two reasons as follow. First, the mass flow rate of working fluid was increased with $T_{h,in}$ resulted in an increase of consumed power of pump, which increment of consumed power in low mole fraction of front fluid was higher than that of high mole fraction of front fluid of the mixtures. Second, increment of the heat transfer rate of high mole fraction of front fluid was higher than that of low mole fraction of front fluid of the mixtures when $T_{h,in}$ higher than 180 ℃. It is noted that only the mixtures R290-based (namely R245fa/R290 and R245fa/R290) have the same optimal mole fraction at the maximal thermal efficiency and specific power.

As shown in Table 5, although the thermal efficiency of R245fa/R134a at optimal mole fraction was higher than that of the mixtures, it was a HFC mixture refrigerant with high GWP. Furthermore, at $T_{h,in} \leq 150$ ℃ the specific power for R600a/R134a were yielded the highest value, which was 0.1 kJ/kg higher than that of R245fa/R134a. With increasing $T_{h,in}$ from 160 to 210 ℃, the considered specific powers for R245fa/R134a and R600a/R290 were substantially increased to the highest value. Compared with the considered specific power of R245fa/R134a, that of R600a/R290 was low between 0.4 and 1.2 kJ/kg. From the above energy analysis, it can be concluded that the R600a/R134a and R600a/R290 at optimal mole fraction can operate with a low GWP and a relatively high specific power comparing to the other mixtures. Compared with the pure fluids, the thermal efficiency and specific power of the mixtures was high.

Table 4 Pure fluid corresponding to thermal efficiency and specific power at evaporating temperature of 70 ℃

$T_{h,in}$		100℃	120℃	140℃	160℃	180℃	200℃	210℃
R245fa	η_I	5.79	5.79	5.80	5.77	5.75	5.72	5.71
	ξ	6.76	12.20	17.83	23.20	28.78	33.90	36.25
R134a	η_I	5.43	5.43	5.42	5.40	5.39	5.36	5.35
	ξ	6.66	12.00	17.39	22.53	26.70	30.94	33.10
R1234yf	η_I	5.20	5.19	5.18	5.17	5.15	5.13	5.12
	ξ	6.70	12.08	17.43	21.37	25.33	29.36	31.41
R290	η_I	5.27	5.25	5.24	5.23	5.22	5.19	5.18
	ξ	6.42	11.57	16.76	21.41	25.39	29.44	31.50
R600a	η_I	5.63	5.63	5.62	5.61	5.59	5.56	5.55
	ξ	6.65	12.00	17.39	22.82	28.16	32.62	34.89

Table 5 Optimal mole fraction (in the round brackets) corresponding to the maximal thermal efficiency and maximal specific power at evaporating temperature of 70 ℃.

$T_{h,in}$		100℃	120℃	140℃	160℃	180℃	200℃	210℃
R245fa/R290	η_I	5.98 (0.41/0.59)	5.97 (0.41/0.59)	5.96 (0.41/0.59)	5.94 (0.41/0.59)	5.92 (0.41/0.59)	5.90 (0.41/0.59)	5.88 (0.41/0.59)
	ξ	7.67 (0.41/0.59)	13.83 (0.41/0.59)	20.03 (0.41/0.59)	25.64 (0.42/0.58)	30.20 (0.42/0.58)	34.84 (0.42/0.58)	37.20 (0.42/0.58)
R245fa/R134a	η_I	6.33 (0.95/0.05)	6.33 (0.95/0.05)	6.32 (0.95/0.05)	6.30 (0.95/0.05)	6.28 (0.95/0.05)	6.25 (0.95/0.05)	6.23 (0.95/0.05)
	ξ	7.87 (0.17/0.83)	14.19 (0.17/0.83)	20.55 (0.17/0.83)	26.96 (0.17/0.83)	32.54 (0.95/0.05)	38.17 (0.95/0.05)	40.74 (0.95/0.05)
R245fa/R1234yf	η_I	6.26 (0.97/0.03)	6.26 (0.97/0.03)	6.25 (0.97/0.03)	6.23 (0.97/0.03)	6.21 (0.97/0.03)	6.18 (0.97/0.03)	6.16 (0.97/0.03)
	ξ	7.87 (0.2/0.8)	14.20 (0.2/0.8)	20.56 (0.2/0.8)	25.96 (0.2/0.8)	32.16 (0.97/0.03)	37.71 (0.97/0.03)	40.25 (0.97/0.03)
R600a/R290	η_I	6.23 (0.81/0.19)	6.22 (0.81/0.19)	6.21 (0.81/0.19)	6.19 (0.81/0.19)	6.17 (0.81/0.19)	6.14 (0.81/0.19)	6.13 (0.81/0.19)
	ξ	7.63 (0.81/0.19)	13.77 (0.81/0.19)	19.94 (0.81/0.19)	26.16 (0.81/0.19)	32.12 (0.81/0.19)	37.03 (0.81/0.19)	39.53 (0.81/0.19)
R600a/R134a	η_I	6.16 (0.94/0.06)	6.15 (0.94/0.06)	6.14 (0.94/0.06)	6.13 (0.94/0.06)	6.11 (0.94/0.06)	6.08 (0.94/0.06)	6.06 (0.94/0.06)
	ξ	7.91 (0.35/0.65)	14.27 (0.35/0.65)	20.66 (0.35/0.65)	25.95 (0.35/0.65)	31.86 (0.94/0.06)	36.73 (0.94/0.06)	39.21 (0.94/0.06)
R600a/R1234yf	η_I	5.93 (0.41/0.59)	5.92 (0.41/0.59)	5.91 (0.41/0.59)	5.90 (0.41/0.59)	5.88 (0.41/0.59)	5.85 (0.41/0.59)	5.83 (0.41/0.59)

ξ	7.38 (0.28/0.72)	13.32 (0.28/0.72)	19.29 (0.28/0.72)	25.30 (0.3/0.7)	30.08 (0.4/0.6)	34.75 (0.4/0.6)	37.13 (0.4/0.6)

Figure 3 illustrates that the thermal efficiency and specific power of the mixtures varying with the heat source temperature at a given evaporating temperature. The results indicate the thermal efficiency and specific power were slightly and notably affected by $T_{h,in}$, respectively. For a given evaporating temperature, the thermal efficiency was slightly decreased with an increase of heat source temperature. By contrast, the specific power was linearly increased with heat source temperature. This was because of outlet temperature of heat source decreased with an increase of $T_{h,in}$ to cause an increase of heat transfer rate in evaporator.

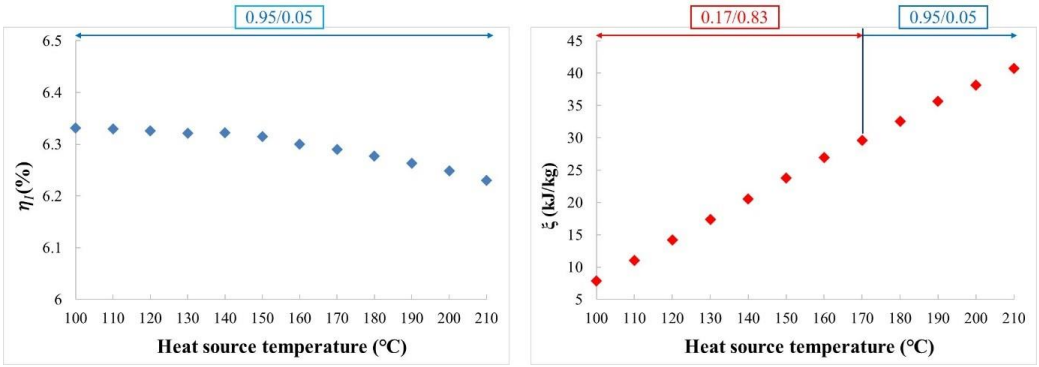

(a) (b)

Fig. 3 (a) the thermal efficiency and (b) specific power for R245fa/R134a at various $T_{h,in}$.

3.2 Effect of the heat source temperature

To investigate the effect of $T_{h,in}$ and optimal mole fraction on change of evaporating pinch point, the trends of $\dot{Q}_h$ and ξ for the mixtures are demonstrated in Figs. 4 and 5, respectively. The results show that the heat transfer rate in the evaporator and specific power was linearly increased with an increase of $T_{h,in}$. Meanwhile, as inlet temperature higher than 180 ℃, the difference of heat transfer rate among the mixtures was reduced. This was because of the evaporating pinch point shifted from state 3 to state 2 which represented the outlet of the feeding pump. As $T_{h,in}$ lower than 170 ℃, for R245fa/R134a, R245fa/R1234yf, R600a/R134a and R600a/R1234yf the front fluid of the mixtures, namely R245fa and R600a, was low mole fraction which the mixture's thermodynamic properties similar to R134a and R1234yf to cause their specific power approached to the same value. By contrast, difference of the specific power among the mixtures was increase at $T_{h,in} \geq 180$ ℃ due to front fluid of the mixtures in high mole fraction.

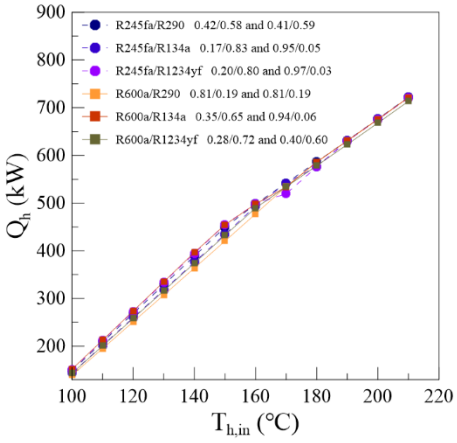

Fig. 4 Effect of $T_{h,in}$ on $\dot{Q}_{hs}$.

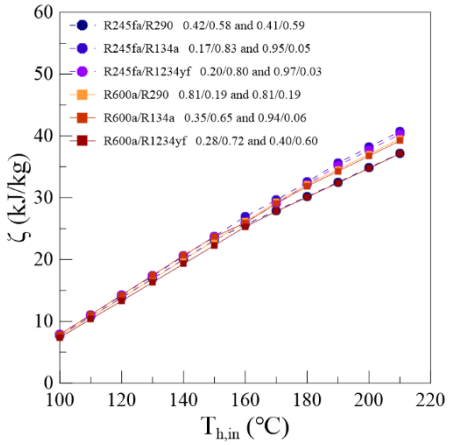

Fig. 5 Effect of $T_{h,in}$ on ξ.

4. CONCLUSIONS

In the present study, the thermodynamic performance of ORC with the mixtures was examined for heat source temperature ranged from 100 to 210 ℃. Mole fraction optimization of the six mixtures corresponding to the maximal thermal efficiency and specific power was performed at various heat

source temperatures. Additionally, the heat transfer rate was compared to analyze shift of evaporating pinch point. The main conclusions can be summarized as follows:

(1) The difference of optimal mole fraction between the maximal thermal efficiency and specific power was existed, except R245fa/R290 and R600a/R290. Optimal mole fraction corresponding to maximal thermal efficiency was not affected by $T_{h,in}$. However, for optimal mole fraction corresponding to maximal specific power the front fluid of mixtures (R245fa and R600a) was changed from low to high mole fraction, when $T_{h,in}$ rose from 170 to 180 ℃, except R245fa/R290 and R600a/R290. Additionally, the thermal efficiency and specific power were slightly and notably affected by $T_{h,in}$, respectively. Moreover, the thermal efficiency was decreased with an increase of $T_{h,in}$ at evaporating temperature of 70 ℃.
(2) When $T_{h,in} \geq 180$ ℃, the specific powers for R245-mixture (R245fa/R134a and R245fa/R1234yf) and R600a-mixture (R600a/R134a and R600a/R1234yf) were approached to R245fa and R600a of pure fluids, respectively, because of the front fluid of the mixtures at high mole fraction.
(3) The R600a/R134a and R600a/R290 at optimal mole fraction can operate with a low GWP and a relatively high specific power comparing to the mixtures. Based on environmentally friendly and acceptable specific power, R600a/R134a and R600a/R290 could be instead of R245fa/R134a.

REFERENCES

Wei, D.H., Lu, X.S., Lu, Z., Gu, J.M., 2007, Performance analysis and optimization of organic Rankine cycle (ORC) for waste heat recovery, Energy Conversion and Management., vol. 48: p. 1113-1119.

Desai, N.B., Bandyopadhyay, S., 2009, Process integration of organic Rankine cycle. Energy., vol. 34: p. 1674-1686.

Papadopoulos, A.I., Stijepovic, M., Linke, P., 2010, On the systematic design and selection of optimal working fluids for Organic Rankine Cycles, *Appl Therm Eng*., vol. 30: p. 760-769.

Dai, Y.P., Wang, J.F., Lin, G., 2009. Parametric optimization and comparative study of organic Rankine cycle (ORC) for low grade waste heat recovery, *Energy Conversion and Management*., vol. 50: p. 576-582.

Xu, H., Gao, N., Zhu, T., Fischer, J., 2016, Investigation on the fluid selection and evaporation parametric optimization for sub- and supercritical organic Rankine cycle, *Energy*., vol. 96: p. 59-68.

Tchanche, B., Papadakis, G., Lambrinos, G., Frangoudakis, A., 2009, Fluid selection for a lowtemperature solar organic Rankine cycle, *Appl Therm Eng*., vol. 29: p. 2468-2476.

Heberle, F., Preiinger, M., Brüggemann, D., 2012, Zeotropic mixtures as working fluids in organic Rankine cycles for low-enthalpy geothermal resources, *Renew Energy*., vol. 37: p.364-370.

Borsukiewicz-Gozdur, A., Nowak, W., 2007, Comparative analysis of natural and synthetic refrigerants in application to low temperature Clausius-Rankine cycle, *Energy*., vol. 32: p. 344-352.

Wang, X., Zhao, L., 2009, Analysis of zeotropic mixtures used in low-temperature solar Rankine cycles for power generation, *Solar Energy*., vol. 83: p.605-613.

Sadeghi, M., Nemati, A., Ghavimi, A., Yari, M., 2016, Experimental investigation on the performance of ORC power system using zeotropic mixture R601a/R600a, *International Journal of Energy Research*., vol. 41: p.611-754.

Wang, Y., Liu, X., Ding, X., Weng, Y., 2016, Thermodynamic analysis and multi-objective optimization of various ORC (organic Rankine cycle) configurations using zeotropic mixtures, *Energy*., vol. 109: p.791-802.

Dong, B., Xu, G., Li, T., Quan, Y., Wen, J., 2018, Thermodynamic and economic analysis of zeotropic mixtures asworking fluids in low temperature organic Rankine cycles, *Applied Thermal Engineering*., vol. 132: p.545-553.

Lemmon, E.W., Huber, M.L., McLinden, M.O., 2010, NIST Standard Reference Database 23: Reference Fluid Thermodynamic and Transport Properties REFPROP, Version 9.0, National Institute of Standards and Technology, Standard Reference Data Program, Gaithersburg, USA.

Le V.L., G. Kheiri A, Feidt M., Pelloux-Prayer S., 2014, Thermodynamic and economic optimizations of a waste heat to power plant driven by a subcritical ORC (Organic Rankine Cycle) using pure or

zeotropic working fluid. Energy., vol. 78: p.622-638.

ACKNOWLEDGMENTS

The authors gratefully acknowledge the financial support provided for this study by the Bureau of Energy of the Republic of China under No. 108-D0103 and Ministry of Science and Technology of the Republic of China under MOST 108-2622-E-006-017-CC1.

NOMENCLATURE

h	specific enthalpy (kJ/kg)
$\dot{m}$	mass flow rate (kg/s)
P	pressure (MPa)
$\dot{Q}$	heat transfer flow rate (kW)
s	specific entropy (kJ kg^{-1} K^{-1})
T	temperature (°C)
$\dot{W}$	power input/output (kW)

Greek letters

η	efficiency (%)
ΔT	temperature difference (°C)

Superscript

elec	electrical
p	pump

Subscript

b	normal boiling point
c	cooling source
cri	critical
cond	condenser/condensation
c,in/c,out	cooling source inlet/outlet
evap	evaporator/evaporation
exp	expander
gen	generator
m	motor
h	heat source
h,in/h,out	heat source inlet/outlet
s	isentropic
net	net
p	pump
pp	pinch point
tot	total
wf	working fluid
I/II	first/second law of thermodynamics
1-7	state point
0	environment state
in/out	inlet/outlet

Acronyms

ODP	ozone depletion potential
GWP	global warming potential